Polymer translocation into laterally unbounded confined environments

Kaifu Luo[1,a)] and Ralf Metzler[2,b)]

[1]*Department of Polymer Science and Engineering, CAS Key Laboratory of Soft Matter Chemistry,*
University of Science and Technology of China, Hefei, Anhui Province 230026, People's Republic of China
[2]*Department of Physics, Technical University of Munich, Garching D-85748, Germany*

Using Langevin dynamics simulations in three dimensions, we investigate the dynamics of polymer translocation into the regions between two parallel plane walls with separation R under a driving force F. Compared with an unconfined environment, the translocation dynamics is greatly changed due to the crowding effect of the partially translocated monomers. The translocation time τ initially decreases rapidly with increasing R and then saturates for larger R, and the confined environment leads to a nonuniversal dependence of τ on F. © 2010 American Institute of Physics.
[doi:10.1063/1.3466922]

I. INTRODUCTION

The transport of biopolymers through a nanopore has attracted broad interest because it is a challenging problem in polymer physics and is also related to many biological processes, such as DNA and RNA translocation across nuclear pores, protein transport through membrane channels, and virus injection.[1] Moreover, the translocation process has been argued to have potentially revolutionary technological applications, including rapid DNA sequencing, gene therapy and controlled drug delivery.[2–8] From both the basic physics as well as a technology design perspective, an important measure is the scaling of the average translocation time τ with the polymer length N, $\tau \sim N^{\alpha}$, and the value of the corresponding scaling exponent α.

For unbiased translocation, standard equilibrium Kramers analysis[9] of diffusion through an entropic barrier yields $\tau \sim N^2$.[10,11] However, as noted by Chuang *et al.*,[12] the quadratic scaling behavior for unbiased translocation cannot be correct for a self-avoiding polymer. The reason is that the translocation time would be shorter than the Rouse equilibration time of a self-avoiding polymer, $\tau_R \sim N^{1+2\nu}$, where the Flory exponent $\nu = 0.588$ in three dimensions (3D) and $\nu_{2D} = 0.75$ in two dimensions (2D).[13–15] This observation renders the concept of equilibrium entropy and the ensuing entropic barrier inappropriate for polymer translocation dynamics. Chuang *et al.*[12] performed numerical simulations with Rouse dynamics for a 2D lattice model to study the translocation for both phantom and self-avoiding polymers. They decoupled the translocation dynamics from the diffusion dynamics outside the pore by imposing the restriction that the first monomer, which is initially placed in the pore, is never allowed to escape back out of the pore. Their results show that for large N, $\alpha = 1 + 2\nu$, which scales in the same manner as the equilibration time but with a considerably larger prefactor. This finding implies the anomalous nature of the translocation dynamics.[16] The exponent $\alpha = 1 + 2\nu$ was corroborated by extensive numerical simulations based on the fluctuating bond (FB)[17] and Langevin dynamics (LD) models with the bead-spring approach.[18,19] Some recent studies[20,21] suggest that the translocation process may be even slower than that dictated by the relaxation time. The accuracy of these claims is questioned in further work.[22]

The passage of a flexible chain through a nanopore involves a large entropic barrier, thus polymer translocation needs driving forces, which can be provided by an external applied electric field in the pore,[18,23–34] a pulling force exerted on the end of a polymer,[23,35,36] binding particles (chaperones),[37,38] or geometrical confinement of the polymer.[39–44]

Most of the studies focus on driven translocation under an external applied electric field in the pore. Standard equilibrium Kramers analysis[9] of diffusion through an entropic barrier yields $\tau \sim N$ (assuming friction to be independent of N).[10,11] Kantor and Kardar[23] demonstrated that the assumption of equilibrium in polymer dynamics breaks down more easily and provided a lower bound $\alpha = 1 + \nu$ for the translocation time by comparison to the unimpeded motion of the polymer. Using FB[24] and LD[18,25] models, a crossover from $\alpha = 2\nu$ for relatively short polymers to $\alpha = 1 + \nu$ for longer chains was found in 2D. Recently, however, alternate scaling scenarios have been presented. For driven translocation, Dubbeldam *et al.*[26] show $\alpha = 1.55$ in 2D and $\alpha = 1.50$ in 3D, while Panja *et al.*[27] find $\alpha = 1.43$ in 2D and $\alpha = 1.37$ in 3D. Obviously, these two views disagree with each other.[28] Most recently, we find that for faster translocation processes $\alpha = 1.37$ in 3D,[22,30] while it crosses over to $\alpha = 1 + \nu$ for slower translocation, corresponding to weak driving forces and/or high friction.[30]

However, the above physical pictures are based on translocation into an unconfined *trans* side. Very little attention is paid to the dynamics of translocation into confined environments. It is known that the crowding due to macromolecular aggregates and other inclusions in the cellular cytoplasm can be as high as 50% by volume and has considerable influence on reaction rates, protein folding rates, and equilibria *in vivo*.[45] Similarly, polymer translocation into a confined envi-

---

a)Author to whom the correspondence should be addressed. Electronic mail: kluo@ustc.edu.cn.
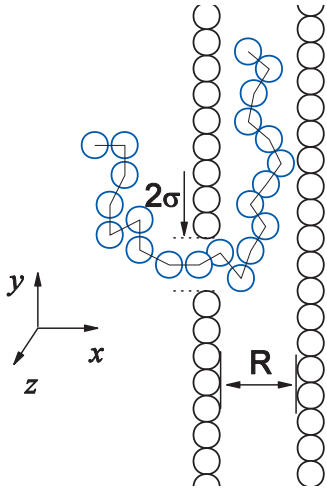b)Electronic mail: metz@ph.tum.de.

FIG. 1. Schematic representation of polymer translocation into a confined environment under an external driving force F in the pore. The simulations are carried out in a planar confinement (3D), where two plates are separated by a distance R. One plate has a pore of length $L=\sigma$ and diameter $W=2\sigma$.
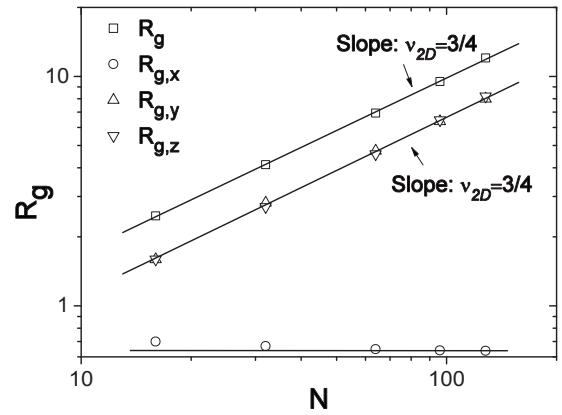

FIG. 2. The radius of gyration at equilibrium state as a function of the chain length confined between two walls with separation $R=3.5$. In the figure, $R_{g,y}=R_{g,z}=R_\parallel$ is the direction parallel to the wall, while $R_{g,x}=R_\perp$ is the direction perpendicular to the wall.

ronment is subject to a large entropic penalty which should dramatically affect the translocation dynamics. In addition, studies on translocation into confined geometries will shed light on the dynamics of DNA packaging.[46]

We here investigate the dynamics of polymer translocation into the region between two parallel plane walls (3D) using Langevin dynamics simulations. The paper is organized as follows. In Sec. II, we briefly describe our model and the simulation technique. In Sec. III, we present our results. Finally, the conclusions and discussion are presented in Sec. IV.

II. MODEL AND METHODS

In our numerical simulations, the polymer chains are modeled as bead-spring chains of Lennard-Jones (LJ) particles with the finite extension nonlinear elastic (FENE) potential. Excluded volume interaction between monomers is modeled by a short range repulsive LJ potential: $U_{LJ}(r)=4\varepsilon[(\sigma/r)^{12}-(\sigma/r)^6]+\varepsilon$ for $r\le 2^{1/6}\sigma$ and 0 for $r>2^{1/6}\sigma$. Here, σ is the diameter of a monomer and ε is the depth of the potential. The connectivity between neighboring monomers is modeled as a FENE spring with $U_{FENE}(r)=-(1/2)kR_0^2\ln(1-r^2/R_0^2)$, where r is the distance between consecutive monomers, k is the spring constant, and R_0 is the maximally allowed separation between connected monomers.

We consider a geometry as shown in Fig. 1, where two walls with separation R are formed by stationary particles within a distance σ from each other. One wall has a pore of diameter 2σ. Between all monomer-wall particle pairs, there exists the same short range repulsive LJ interaction as described above. In the Langevin dynamics simulation, each monomer is subjected to conservative, frictional, and random forces, respectively, with[47] $m\ddot{\mathbf{r}}_i=-\nabla(U_{LJ}+U_{FENE})+\mathbf{F}_{ext}-\xi\mathbf{v}_i+\mathbf{F}_i^R$, where m is the monomer's mass, ξ is the friction coefficient, $\mathbf{v}_i$ is the monomer's velocity, and $\mathbf{F}_i^R$ is the random force which satisfies the fluctuation-dissipation theorem. The external force is expressed as $\mathbf{F}_{ext}=F\hat{x}$, where F is the exter-

nal force strength exerted exclusively on the monomers in the pore, and $\hat{x}$ is a unit vector in the direction along the pore axis. We should mention that in our model the polymer-pore interactions are neglected, which play a very important role in translocation dynamics.[48]

In the present work, we use the LJ parameters ε and σ and the monomer mass m to fix the energy, length, and mass scales, respectively. The time scale is then given by $t_{LJ}=(m\sigma^2/\varepsilon)^{1/2}$. The dimensionless parameters in our simulations are $R_0=2$, $k=7$, $\xi=0.7$, and $k_BT=1.2$ unless otherwise stated. The driving force F is set between 0.5 and 15, which corresponds to the range of voltages used in the experiments.[2,3] The Langevin equation is integrated in time by a method described by Ermak and Buckholz[49] in 3D.

Initially, the first monomer of the chain is placed in the entrance of the pore, while the remaining monomers are undergoing thermal collisions described by the Langevin thermostat to obtain an equilibrium configuration. Typically, we average our data over 1000 independent runs.

III. RESULTS AND DISCUSSION

According to the blob picture,[13] a chain confined between two parallel plates with separation $\sigma\ll R\ll R_g$ will form a 2D self-avoiding walk consisting of n_b blobs of size R. Each blob contains $g=(R/\sigma)^{1/\nu}$ monomers and the number of blobs is $n_b=N/g=N(\sigma/R)^{1/\nu}$. Thus, the blob picture predicts the longitudinal size of the polymer to be[13,14] $R_\parallel\sim n_b^{\nu_{2D}}R\sim N^{\nu_{2D}}\sigma(\sigma/R)^{\nu_{2D}/\nu-1}\sim N^{3/4}\sigma(\sigma/R)^{0.28}$, where the Flory exponent $\nu_{2D}=0.75$ in 2D and $\nu=0.588$ in 3D. Figure 2 shows the radius of gyration as a function of the chain length with wall separation $R=4.5$. We confirm $R_{g,y}=R_{g,z}=R_\parallel\sim N^{\nu_{2D}}\sim N^{3/4}$. $R_{g,x}$ almost does not change with N, but R_g also scales with N in the same way as $R_\parallel$. The R dependence of $R_\parallel$ is shown in Fig. 3, where $R_{g,y}=R_{g,z}=R_\parallel\sim(1/R)^{\nu_{2D}/\nu-1}\sim(1/R)^{0.28}$. For $10.0\ge R\ge 2.5$, $R_{g,x}$ shows linear behavior with R, but $R_g\sim R^{-0.28}$.

The longitudinal relaxation time $\tau_\parallel$ is defined as the time for a polymer moving a distance of order of its longitudinal size, $R_\parallel$. Thus, $\tau_\parallel$ scales as $\tau_\parallel\sim(R_\parallel^2/\tilde{D})\sim N^{1+2\nu_{2D}}R^{2(1-\nu_{2D}/\nu)}\sim N^{2.50}R^{-0.55}$, where σ is the segment length and $\tilde{D}\sim 1/N$ is
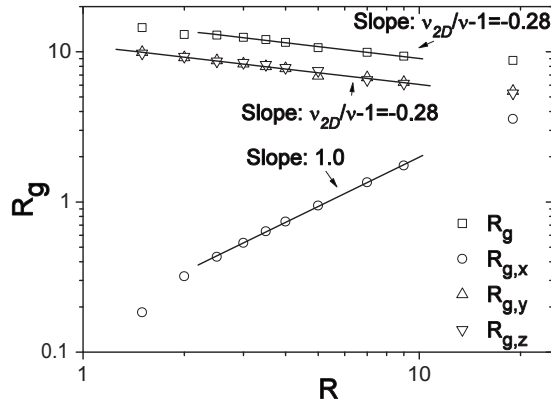
FIG. 3. The radius of gyration at equilibrium state under the confinementi between two walls with separation R for $N=128$. In the figure, $R_{g,y}=R_{g,z}=R_\parallel$ is in the direction parallel to the wall, while $R_{g,x}=R_\perp$ is in the direction perpendicular to the wall.

the diffusion constant. The free energy cost of the confined chain in units of $k_B T$ is simply the number of the blobs, $\mathcal{F}=N(\sigma/R)^{1/\nu}$.

For polymer translocation into confined environments, a driving force is necessary to overcome the entropic repulsion $f(R)$ exerted by already translocated monomers. Due to the highly nonequilibrium property of the translocation process, it is difficult to estimate the resisting force $f(R)$. For polymer translocation into the region between two parallel plane walls with separation R, we assume that the resisting force $f(R)$ scales as $f(R)=CR^\gamma$ for slow translocation processes, with C and γ being the prefactor and the scaling exponent, respectively. Then, under an external driving force F in the pore the translocation time τ can be written as $\tau \sim (N^\alpha/F -f(R)) \sim (N^\alpha/F(1-CR^\gamma/F))$ with α being the scaling exponent of τ with chain length N. Due to $\tau_\infty \sim (N^\alpha/F)$ for the unconfined system with $R \sim \infty$ for slow translocation processes, we have $1-(\tau_\infty/\tau) \sim CR^\gamma/F$. Based on this relationship, we can examine the dependence of τ on R.

A. Translocation times as a function of the chain length

Figure 4 shows the translocation time τ as a function of the chain length N. For a strong driving force $F=5$, we find
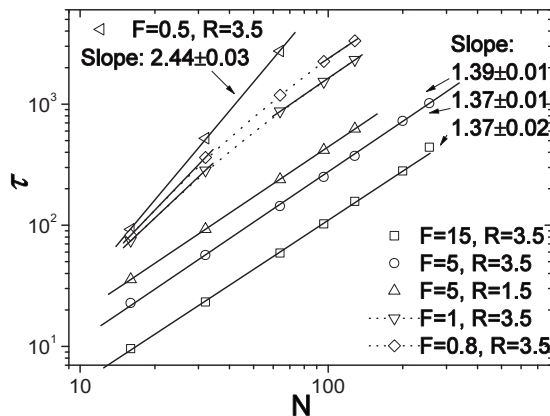

FIG. 4. Translocation time τ as a function of the chain length N for different R and F in 3D.
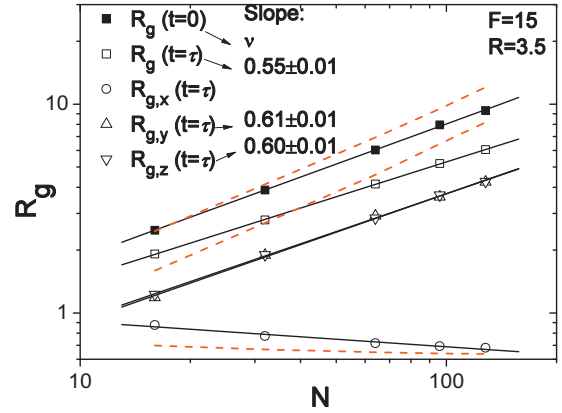

FIG. 5. The radius of gyration of the chain before translocation ($t=0$) and at the moment just after the translocation ($t=\tau$) for $F=15$ and $R=3.5$. Here, the x direction is perpendicular to the wall, while y and z are along the wall. The dashed lines are equilibrium values of R_g, $R_\parallel$, and R_x for chains confined between two walls, as shown in Fig. 2.

$\tau \sim N^\alpha$ with $\alpha=1.39 \pm 0.01$ and 1.37 ± 0.01 for $R=3.5$ and 1.5, respectively, which are quite close to that for an unconfined system ($R=\infty$).[22,31,32,44] For the case with very strong driving force $F=15$ and $R=3.5$, the scaling exponent also does not change, $\alpha=1.37 \pm 0.02$. We have checked the translocation velocity with respect to the last monomer and found $v \sim N^\beta$ with $\beta \approx -0.8$, which is also the same as that for an unconfined system.[31,44] Under a planar confinement, during the translocation process the translocated monomers cannot have time to diffuse away from the pore corresponding to a pronounced nonequilibrium situation. After the translocation the distance the last monomer has moved is always the radius of the gyration of a chain $R_g \sim N^\nu \sigma$ for its unconfined state. Thus, the translocation time can be estimated by $\tau \sim (R_g/v)$, which is confirmed by our numerical results.

The above scaling behavior can be understood by measuring the radius of gyration of the chain before translocation and at the moment just after the translocation, as shown in Fig. 5. For the chain at the moment just after the translocation, $R_g \sim N^{0.55}$ and $R_{g\parallel} \sim N^{0.60}$, significantly lower than their equilibrium values and different from the equilibrium scaling of $N^{3/4}$ as shown in Fig. 2. These results indicate a pronouncedly nonequilibrium compression of the chain immediately after translocation, as shown in Fig. 6.

With decreasing the driving force to $F=1.0$ and 0.8, the scaling exponent remains the same only for longer chains. For shorter chains $N \leq 32$, the translocation is much faster due to considerably lower confinement.

Decreasing the driving force further to $F=0.5$, we find the translocation dynamics crosses over to another regime with $\alpha=2.44 \pm 0.03$ at least for $N \leq 64$. For longer chains, the computation is very expensive due to lower translocation probability and a longer translocation time. This result is completely different compared with the case without the planar confinement ($R=\infty$), where we have found $\tau \sim N^{1+\nu}$ for $F=0.5$ in our previous studies.[30] Without the planar confinement, the previous prediction by Chuang et al.[12] shows that the translocation time scales in the same way as the relaxation time of the chain for unbiased translocation. Here, our exponent $\alpha=2.44 \pm 0.03$ for $F=0.5$ is very close to 2.50,
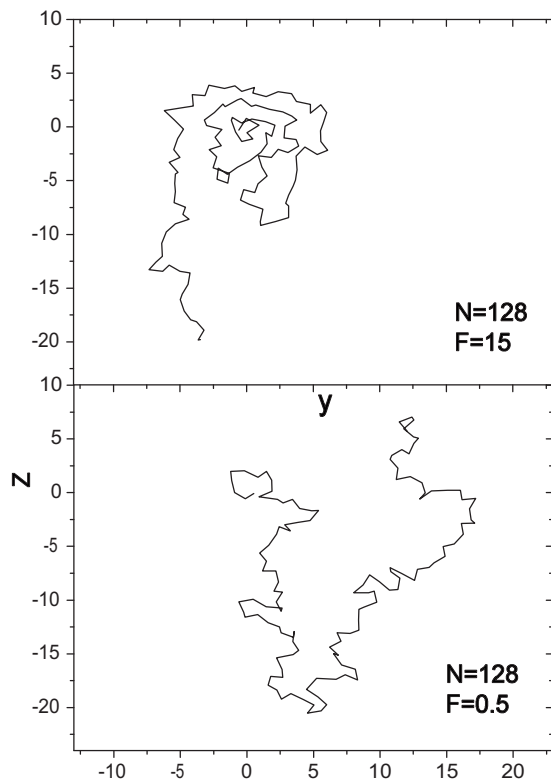
FIG. 6. The chain conformation projected onto the yz plane for $N=128$ under strong and weak driving forces, respectively.

which demonstrates that τ scales in the same way as the 2D longitudinal relaxation time for the weak driving force. The reason is that the weak driving force F is almost balanced by the resisting force due to the confinement entropy and the net driving force is close to zero. Compared with strong driving cases, the chain conformation is not so compressed, as shown in Fig. 6. Here, we also should point out that the exponent $\alpha=2.44$ is a little smaller than 2.50 due to the fact that during the translocation process the untranslocated monomers are not confined. To obtain the exponent 2.5, one should initially squeeze the whole chain into the confined spaces between two plates and then record the time during the chain moving a distance of order of $R_{\parallel}$.

B. Translocation times as a function of R

Figure 7 shows the R dependence of the translocation time for $F=5.0$ and $N=128$. Initially, τ decreases rapidly with increasing R and then almost saturates for larger R. Quantitatively, we check $1-(\tau_{\infty}/\tau)$ as a function of R, see the insert of Fig. 7. For $R\leq3$, we find $\gamma=-1.61\pm0.06$. It is close to the exponent $-1/\nu=-1.70$, which is the theoretical value for equilibrium translocation processes with $f(R)\sim R^{-1/\nu}$. This result also shows that for $R\leq3$, the chains really feel strong confinement and the translocation is slow enough for the chain to be close to local equilibrium. Figure 8 shows the radius of gyration of the chain as a function of R at the moment after the translocation. We find $R_{g,y}=R_{g,z}\sim R^{-0.20}$ for $R<9$, which is slightly lower than the equilibrium exponent -0.28. In addition $R_{g,x}\sim R^{1.43}$ for $R\leq3$, somewhat lower than the equilibrium exponent $1/\nu=1.70$. For larger R, such as $R=19$, $R_{g,x}=R_{g,y}=R_{g,z}$.

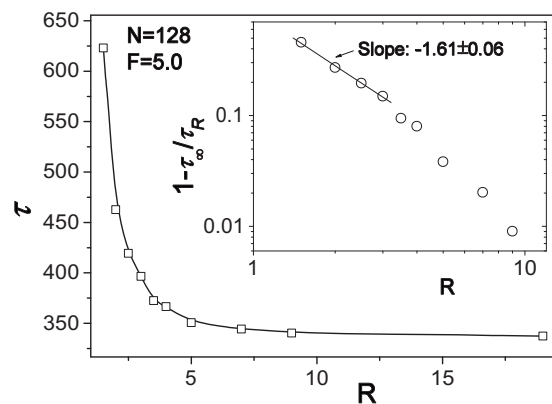FIG. 7. Translocation time τ as a function of R for chain length $N=128$ under $F=5$ in 3D.

C. Translocation times as a function of the driving force

According to the Langevin equation, when the inertia term can be neglected, the balance of the frictional force and the driving force, $\xi v=F$, gives $\tau\sim\xi/F$ for the case without planar confinements. The Langevin dynamics simulation results[18,30] confirm $\tau\sim1/F$ only for slow translocation with lower values of F/ξ. For fast translocation with higher values of F/ξ, we have found $\tau\sim F^{-0.8}$ due to the highly deformed chain conformation on the trans side, reflecting a pronounced nonequilibrium situation.[30] Figure 9 shows the plot of τ as function of F for translocation into a region of a planar confinement. Under strong driving forces, such as $F\geq5$, compared with the case without confinement $\tau\sim F^{-0.80\pm0.02}$ is still observed. Under a planar confinement, it is more difficult for translocated monomers to diffuse away from the pore, which slows down the translocation. As a result, the exponent must be lower than -1. Under weak driving forces $F\leq2.5$, we find $\tau\sim F^{-1.25\pm0.03}$. For translocation into two parallel plates with separation R, the effective driving force is $F(1-Cf(R)/F)$. For weaker driving forces, the resisting force $f(R)$ becomes more and more important because $(1-Cf(R)/F)$ is closer to zero. Therefore, with decreasing F the translocation is greatly slowed down, resulting
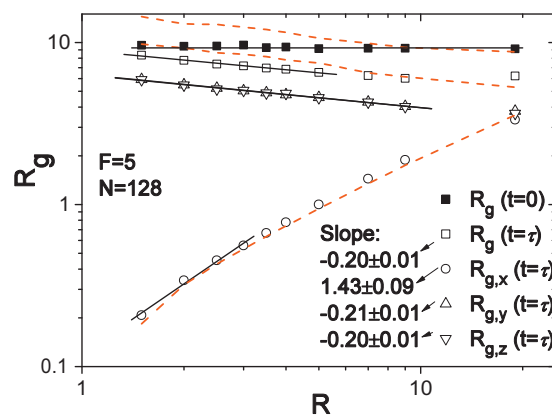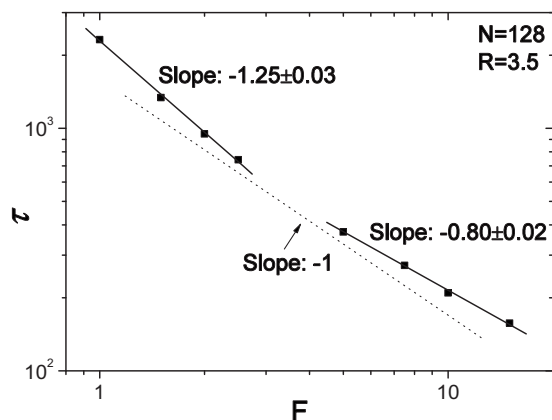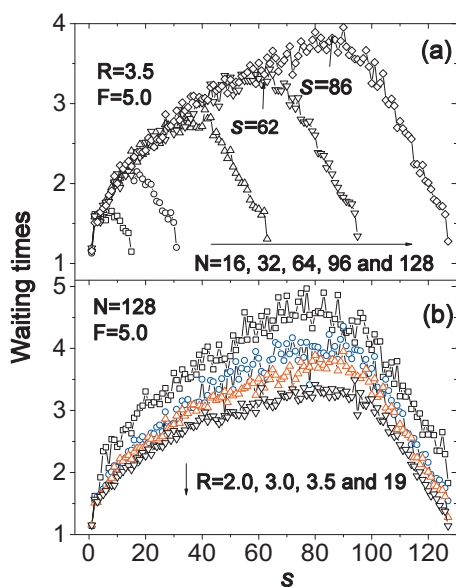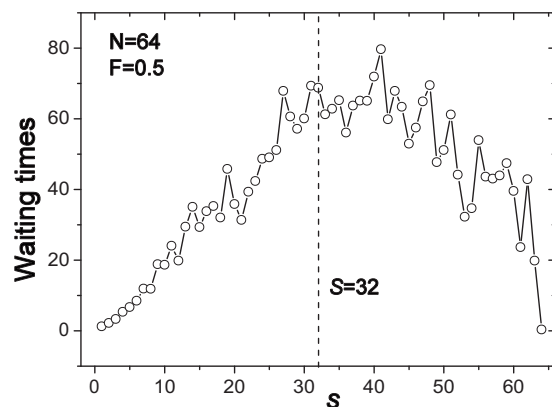

FIG. 8. The radius of gyration of the chain before translocation ($t=0$) and at the moment just after the translocation ($t=\tau$) for $N=128$, $F=5$, and different R. Here, the x direction is perpendicular to the wall, and y and z are along the wall. The dashed lines are equilibrium values of R_g, $R_{\parallel}$, and R_x for chains confined between two walls, as shown in Fig. 3.

FIG. 9. Translocation time τ as a function of F for $N=128$ and $R=3.5$ in 3D.

FIG. 11. Waiting time distribution for $F=0.5$ and $N=64$.

in stronger dependence of τ on F. In our previous results,[48] we find that the polymer-pore interactions can also lead to this behavior.

D. Waiting time distribution

The time of an individual segment passing through the pore during translocation is an important quantity considerably affected by the translocation dynamics. The nonequilibrium nature of translocation has a significant effect on it. We have numerically calculated the waiting times for all monomers in a chain of length N. We define the waiting time of monomer s as the average time between the events that monomer s and monomer $s+1$ exit the pore. Figure 10(a) shows the waiting time distributions for different chain lengths for $R=3.5$ and $F=5$. One obvious feature is that before reaching their maxima the waiting times almost follow the same pathway, which is dominated by the strong driving force. In addition, the maxima occur at $s_{max}>N/2$, such as $s_{max}\approx 0.65N$ and $0.67N$ for $N=96$ and 128, respectively. Figure 10(b) shows the waiting time distributions for $N=128$ and $F=5$ for different R. As expected, with decreasing R, the waiting times increase. Figure 11 shows the waiting time

distributions for $N=64$ and $R=3.5$ under the weak driving force $F=0.5$. After half of the polymer has been translocated, it still takes a considerably long time to exit the pore for the remaining monomers, compared with strong driving cases shown in Fig. 10. This implies different translocation dynamics in the two regimes.

IV. CONCLUSIONS

Using Langevin dynamics simulations, we investigate the dynamics of polymer translocation into the region between two parallel plane walls with separation R. Compared with the chain passage into an unconfined environment, the translocation dynamics is greatly changed. In particular, the translocation time τ initially decreases rapidly with R and then saturates for larger R in 3D, and the confined environment leads to nonuniversal dependence of τ as a function of the driving force. For polymer translocation into 3D confinements with $R=3.5$, we find that under the weak driving force $F=0.5$ the translocation time τ scales with chain length N as $\tau\sim N^{2.44}$, which is in the same manner as the relaxation time of a chain under a planar confinement, while it crosses over to N as $\tau\sim N^{1.39}$ for fast translocation. These behaviors are interpreted by the waiting time of individual monomers.

By systematically treating the entropic penalty due to randomly distributed spherical obstacles (crowding), Gopinathan and Kim[43] demonstrate that the translocation dynamics are significantly altered, resulting in novel scaling behaviors of the translocation time. Depending on the extent of crowding, transmembrane chemical potential asymmetry, and polymer length, there are new and qualitatively different translocation regimes. Therefore, for this kind of crowding environment, translocation dynamics is also expected to be changed under an external applied electric field in the pore.

FIG. 10. Waiting time distribution for different (a) N and (b) R.

[1] B. Alberts, D. Bray, J. Lewis, M. Raff, and J. D. Watson, *Molecular Biology of the Cell* (Garland, New York, NY, 1994).

[2] J. J. Kasianowicz, E. Brandin, D. Branton, and D. W. Deamer, Proc. Natl. Acad. Sci. U.S.A. **93**, 13770 (1996).

[3] A. Meller, J. Phys.: Condens. Matter **15**, R581 (2003); A. Meller, L. Nivon, E. Brandin, J. A. Golovchenko, and D. Branton, Proc. Natl. Acad. Sci. U.S.A. **97**, 1079 (2000); A. Meller, L. Nivon, and D. Branton, Phys. Rev. Lett. **86**, 3435 (2001).

[4] M. Akeson, D. Branton, J. J. Kasianowicz, E. Brandin, and D. W. Deamer, Biophys. J. **77**, 3227 (1999).

[5] S. M. Iqbal, D. Akin, and R. Bashir, Nat. Nanotechnol. **2**, 243 (2007).

[6] J. Clarke, H. C. Wu, L. Jayasinghe, A. Patel, S. Reid, and H. Bayley, Nat. Biotechnol. **4**, 265 (2009).

[7] D. Branton, D. W. Deamer, A. Marziali, H. Bayley, S. A. Benner, T. Butler, M. Di Ventra, S. Garaj, A. Hibbs, X. H. Huang, S. B. Jovanovich, P. S. Krstic, S. Lindsay, X. S. S. Ling, C. H. Mastrangelo, A. Meller, J. S. Oliver, Y. V. Pershin, J. M. Ramsey, R. Riehn, G. V. Soni, V. Tabard-Cossa, M. Wanunu, M. Wiggin, and J. A. Schloss, Nat. Biotechnol. **26**, 1146 (2008).

[8] A. J. Storm, C. Storm, J. Chen, H. Zandbergen, J.-F. Joanny, and C. Dekker, Nano Lett. **5**, 1193 (2005).

[9] H. A. Kramers, Physica (Amsterdam) **7**, 284 (1940).

[10] W. Sung and P. J. Park, Phys. Rev. Lett. **77**, 783 (1996).

[11] M. Muthukumar, J. Chem. Phys. **111**, 10371 (1999).

[12] J. Chuang, Y. Kantor, and M. Kardar, Phys. Rev. E **65**, 011802 (2002).

[13] P. G. de Gennes, *Scaling Concepts in Polymer Physics* (Cornell University Press, Ithaca, NY, 1979).

[14] M. Doi and S. F. Edwards, *The Theory of Polymer Dynamics* (Clarendon, Oxford, 1986).

[15] M. Rubinstein and R. Colby, *Polymer Physics* (Oxford University Press, Oxford, 2003).

[16] R. Metzler and J. Klafter, Biophys. J. **85**, 2776 (2003); Phys. Rep. **339**, 1 (2000).

[17] K. Luo, T. Ala-Nissila, and S. C. Ying, J. Chem. Phys. **124**, 034714 (2006).

[18] I. Huopaniemi, K. Luo, T. Ala-Nissila, and S. C. Ying, J. Chem. Phys. **125**, 124901 (2006).

[19] D. Wei, W. Yang, X. Jin, and Q. Liao, J. Chem. Phys. **126**, 204901 (2007).

[20] D. Panja, G. T. Barkema, and R. C. Ball, J. Phys.: Condens. Matter **19**, 432202 (2007).

[21] J. L. A. Dubbeldam, A. Milchev, V. G. Rostiashvili, and T. A. Vilgis, Phys. Rev. E **76**, 010801(R) (2007).

[22] K. Luo, S. T. T. Ollila, I. Huopaniemi, T. Ala-Nissila, P. Pomorski, M. Karttunen, S. C. Ying, and A. Bhattacharya, Phys. Rev. E **78**, 050901(R) (2008).

[23] Y. Kantor and M. Kardar, Phys. Rev. E **69**, 021806 (2004).

[24] K. Luo, I. Huopaniemi, T. Ala-Nissila, and S. C. Ying, J. Chem. Phys. **124**, 114704 (2006).

[25] K. Luo, T. Ala-Nissila, S. C. Ying, and A. Bhattacharya, J. Chem. Phys. **126**, 145101 (2007).

[26] J. L. A. Dubbeldam, A. Milchev, V. G. Rostiashvili, and T. A. Vilgis, Europhys. Lett. **79**, 18002 (2007).

[27] H. Vocks, D. Panja, G. T. Barkema, and R. C. Ball, J. Phys.: Condens. Matter **20**, 095224 (2008).

[28] J. L. A. Dubbeldam, A. Milchev, V. G. Rostiashvili, and T. A. Vilgis, J. Phys.: Condens. Matter **21**, 098001 (2009).

[29] M. G. Gauthier and G. W. Slater, J. Chem. Phys. **128**, 205103 (2008).

[30] K. Luo, T. Ala-Nissila, S. C. Ying, and R. Metzler, EPL **88**, 68006 (2009).

[31] A. Bhattacharya, W. H. Morrison, K. Luo, T. Ala-Nissila, S. C. Ying, A. Milchev, and K. Binder, Eur. Phys. J. E **29**, 423 (2009); A. Bhattacharya and K. Binder, Phys. Rev. E **81**, 041804 (2010).

[32] T. Sakaue, Phys. Rev. E **76**, 021803 (2007); **81**, 041808 (2010).

[33] Y. D. He, H. J. Qian, Z. Y. Lu, and Z. S. Li, Polymer **48**, 3601 (2007); Y. C. Chen, C. Wang, and M. Luo, J. Chem. Phys. **127**, 044904 (2007); Y. J. Xie, H. Y. Yang, H. T. Yu, Q. W. Shi, X. P. Wang, and J. Chen, *ibid.* **124**, 174906 (2006); M. B. Luo, Polymer **48**, 7679 (2007); T. Sun, L. Zhang, and J. Sun, J. Chem. Phys. **125**, 034702 (2006).

[34] T. Ambjörnsson, S. P. Apell, Z. Konkoli, E. A. DiMarzio, and J. J. Kasianowicz, J. Chem. Phys. **117**, 4063 (2002).

[35] I. Huopaniemi, K. Luo, T. Ala-Nissila, and S. C. Ying, Phys. Rev. E **75**, 061912 (2007).

[36] S. T. T. Ollila, K. F. Luo, T. Ala-Nissila, and S. C. Ying, Eur. Phys. J. E **28**, 385 (2009).

[37] T. Ambjörnsson and R. Metzler, Phys. Biol. **1**, 77 (2004); T. Ambjörnsson, M. A. Lomholt, and R. Metzler, J. Phys.: Condens. Matter **17**, S3945 (2005).

[38] R. Zandi, D. Reguera, J. Rudnick, and W. M. Gelbart, Proc. Natl. Acad. Sci. U.S.A. **100**, 8649 (2003).

[39] P. J. Park and W. Sung, J. Chem. Phys. **108**, 3013 (1998).

[40] M. Muthukumar, Phys. Rev. Lett. **86**, 3188 (2001); J. Chem. Phys. **118**, 5174 (2003).

[41] A. Cacciuto and E. Luijten, Phys. Rev. Lett. **96**, 238104 (2006).

[42] D. Panja, G. T. Barkema, and R. C. Ball, J. Phys.: Condens. Matter **20**, 075101 (2008).

[43] A. Gopinathan and Y. W. Kim, Phys. Rev. Lett. **99**, 228106 (2007).

[44] K. Luo, R. Metzler, T. Ala-Nissila, and S. C. Ying, Phys. Rev. E **80**, 021907 (2009).

[45] J. A. Dix and A. S. Verkman, Annu. Rev. Biophys. **37**, 247 (2008); H. X. Zhou, G. Rivas, and A. P. Minton, *ibid.* **37**, 375 (2008).

[46] D. E. Smith, S. J. Tans, S. B. Smith, S. Grimes, D. E. Anderson, and C. Bustamante, Nature (London) **413**, 748 (2001); I. Ali, D. Marenduzzo, and J. M. Yeomans, J. Chem. Phys. **121**, 8635 (2004).

[47] M. P. Allen and D. J. Tildesley, *Computer Simulation of Liquids* (Oxford University Press, Oxford, 1987).

[48] K. Luo, T. Ala-Nissila, S. C. Ying, and A. Bhattacharya, Phys. Rev. Lett. **99**, 148102 (2007); **100**, 058101 (2008); Phys. Rev. E **78**, 061918 (2008); **78**, 061911 (2008).

[49] D. L. Ermak and H. Buckholz, J. Comput. Phys. **35**, 169 (1980).